

Dynamic Decoupling and Molecular Complexity of Glass-Forming Maltitol

L. Carpentier* and M. Descamps

Laboratoire de Dynamique et Structure des Matériaux Moléculaire, U.M.R. CNRS 8024, Bât. P5, Ust Lille, 59655 Villeneuve d'Ascq, France

Received: July 11, 2002; In Final Form: October 29, 2002

A low frequency dielectric study of glass-forming maltitol and sorbitol has been performed. It enables us to show an effect of a side branching on the sub- T_g relaxation curves. This molecular complexity has no effect on the temperature evolution of the secondary relaxation times of both compounds, which superimpose perfectly. However, side branching leads in maltitol to a sharpening of the corresponding distribution and occurrence of an intermediate strongly activated process, which has no separate secondary counterpart.

I. Introduction

The calorimetric glass transition (at T_g) is usually understood as a direct consequence from a competition between the structural relaxation times and the experimental times. However, the evolution of the relaxation processes near and below T_g is far from being simple and is actually a matter of active debate. Well-described but poorly understood is the tendency of the main α process to dramatically slow near T_g . The question of molecular significance and the possible universal nature of a secondary weakly activated β process is also challenging.^{1,2} The decoupling of the relaxations in α and β processes is quite universally observed in the most fragile glass formers such as simple molecular liquids,^{3–5} polymeric systems,^{6,7} glass-forming liquid crystals,⁸ and possibly glassy crystals.^{5,9} It has been argued that the β process could be sometimes attributed to excitations of molecular side groups and sometimes to specific activation of the same species as those involved in the α process. Additional complexities were sometimes revealed such as the appearance of serial decoupling of relaxation modes when investigating the same glass former with different techniques¹⁰ or the emergence of plural sets of α and β processes¹¹ even when working with the same technique. As an experimental contribution to this problem, we present a dielectric study of two polyols of related structure: maltitol and sorbitol. These carbohydrates are widely used in pharmaceutical and dietary foods. They are very suitable for investigating glass formation since both liquids resist against parasitic recrystallization at usual cooling rates. For these two compounds, the molecular mobility has been measured over a wide range of time and temperature using NMR,¹² dielectric¹³ and mechanical relaxation techniques,¹⁴ and viscosity measurements.¹⁵ We display in maltitol the existence of a dynamic process below the glass transition temperature in addition to the β process commonly observed in most glass-forming materials. Furthermore, the evolution of α processes evaluated by dielectric relaxation cannot be followed at low frequency due to an important contribution related to conductivity phenomena. To circumvent this problem, we present results obtained by using the recent technique of temperature-modulated differential scanning calorimetry (TMDSC), which allows us to determine characteristic relaxation times in a temperature range immediately above the glass transition temperature. Concerning the specific α – β decoupling problem, the parallel investigation of both compounds shows a lot of

advantages to shed light on the influence of molecular complexity. They are fragile glass formers,^{16–19} which increase the possibilities to separate and analyze the different relaxation processes. Their molecular structures differ by the presence, in maltitol, of a heterocycle branched on the aliphatic chain (Figure 4 inset); this will help to identify the influence of side groups on the dynamical decoupling. Furthermore, sorbitol has been shown recently to exhibit a relatively large contribution of the secondary β process.^{13,16,20,21}

II. Experimental Section

Highly purified crystalline powder of maltitol and sorbitol was obtained from Aldrich Chemicals. Because of their easy tendency to become hydrated, both compounds were first dried under vacuum. The dielectric measurements were performed with the analyzer DEA 2970 of TA Instruments, providing more than seven decades of frequency (1 mHz to 300 kHz), and thus facilitating a complete assessment of the glass behavior (conventions usually fix the characteristic frequency $\nu(T_g) \cong 10$ mHz.) The dielectric cell consisted of an interdigitated array of electrodes on which the samples were melted (T_m (maltitol) $\cong 420$ K – T_m (sorbitol) $\cong 380$ K). This allowed an optimal filling of the cell. The samples were also subjected to a constant compressive force during the experiments, which ensured that the sensor maintained good contact with the sample even if the sample hardened. During the experiments, the dielectric cell was protected against the room atmosphere and a dried airflow minimized hydration of the sample. A nitrogen cooling device provided testing capability from 120 to 700 K. Two kinds of experiments were performed, isochronal measurements to obtain a general overview of the different relaxation processes and isothermal measurements to obtain a more precise description of relaxations in the glassy state. Ramp and heating methods were selectable at rates from 0.01 to 50 K. In isothermal processes, the temperature was controlled to within 0.01 K.

For the calorimetric measurements, a modulated DSC 2920 TA instruments equipped with a refrigerated cooling system (RCS) was used. This technique has been shown to be able to provide a specific heat spectroscopic analysis of the enthalpy relaxation in the vicinity of T_g .²² The samples were encapsulated in aluminum-crimped pans. The samples weight was in the range of 7–10 mg, which was a low enough value to allow the sample to follow the imposed thermal oscillations. The temperature and

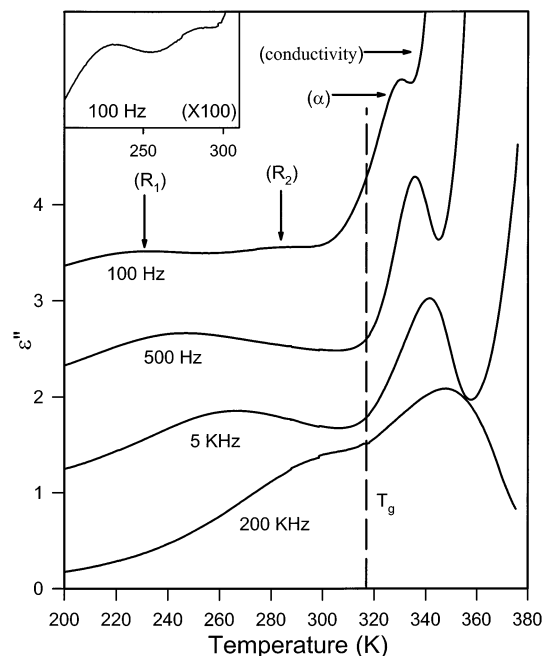


Figure 1. Isochronal imaginary part of the dielectric response plotted against the temperature for four typical frequencies. Each curve is shifted upward by adding 1.0 (respectively, 2.0 and 3.0) to the measured ϵ'' . Data are taken on cooling with a sweeping rate of 1 K/min. The inset shows a closed view of the sub- T_g 100 Hz isochronal measurement.

enthalpy were calibrated using indium as a standard, and the complex heat capacity was calibrated from the measurement of the complex heat capacity of sapphire in the studied temperature range.

III. Isochronal Measurements in Maltitol

A. Dielectric Analysis. A first isochronal analysis of the dielectric susceptibility of maltitol provides a general overview of the different relaxation processes, which occur in the metastable and glassy states ($T_g \approx 313$ K²³). Measurements span a broad domain of temperatures from 390 to 150 K and a frequency range from 0.5 Hz to 300 kHz. They have been performed with a sweeping rate of 1 K/min. Figure 1 shows the imaginary part (ϵ'') of the dielectric susceptibility as a function of temperature for frequencies of 100 Hz, 500 Hz, 5 kHz, and 200 kHz. The typical features revealed by these isochronal evolutions are the following:

(i) A step rise of ϵ'' at the higher temperatures, which is clearly related to the ionic conductivity. (ii) A rather sharp and asymmetric relaxation peak situated above the thermodynamic glass transition exhibits the common characteristics of the α primary relaxation process found in amorphous polymers²⁴ and in rigid molecular glasses.^{25,26} Its maximum only slightly shifts with the frequency. At lower frequencies (below 100 Hz), this α peak is completely hidden by the conductivity contribution. The limited shift of the peak maximum with temperature demonstrates the rapid increase of the mean relaxation time as the glass transition is approached. It thus indicates that maltitol belongs to the fragile liquids class.²⁷ (iii) A very broad and nearly symmetrical sub- T_g relaxation peak is best identified in the intermediate frequency range (500 Hz to 5 kHz). At 5 kHz, the magnitude of this secondary peak is only two times smaller than the α peak. Maltitol thus shares with sorbitol the property to be a nonpolymeric compound, which has a secondary peak of exceptionally large amplitude. This peak shifts more rapidly with frequency than the α peak. These two contributions

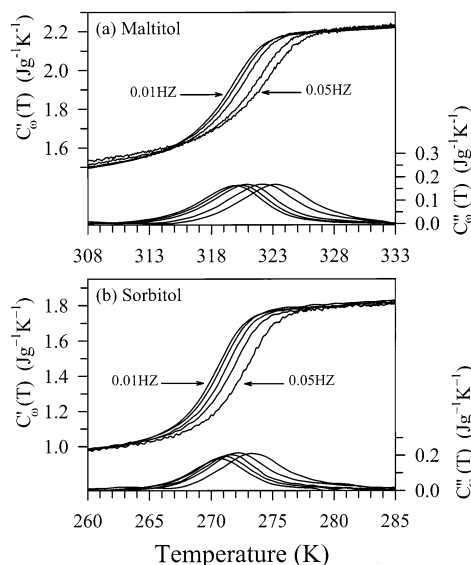


Figure 2. Real and imaginary parts of the complex heat capacity C_{po}^* (T) for (a) maltitol and (b) sorbitol as a function of temperature at different frequencies in the range of 0.01–0.05 Hz (linear rate $q = -0.1$ K min⁻¹).

correspond to very different activation energies. A consequence is that both relaxations merge at higher frequency to give only one shoulder on the low-temperature side of the upper temperature process (200 kHz in Figure 1). This merging and the noticeable high-temperature conductivity contribution make the primary dielectric α relaxation data of maltitol only accessible within a restricted frequency range. Another consequence is that isothermal investigations of the dielectric response $\epsilon^*(\omega)$ associated to the α process are not possible. (iv) An outstanding feature of the lowest frequency curves (100 Hz in Figure 1) is the splitting of the broad sub- T_g bump in two low-amplitude peaks. The two corresponding processes are hereafter referred as R_1 and R_2 relaxations. While R_1 appears to be roughly the low-temperature extension of the broad secondary process observed at higher frequency, the merging R_2 peak occurs at higher temperature and thus reveals a dielectric process that survives in the glassy state with a rather high activation energy.

B. TMDSC Analysis. It has been shown²² that TMDSC gives the possibility to perform specific heat spectroscopy analysis on one decade of frequency in a range (0.01–0.1 Hz) that allows us to investigate the dynamics of glass-forming liquids just above the transformation domain of the glasses. The theoretical description of this technique is developed in several papers to which the reader can refer.^{28–30} It allows access to a complex heat capacity $C_{po}^*(T)$ whose reliability to give dynamic information has been demonstrated by comparison with dielectric spectroscopy.³¹ Figure 2 shows the real $C'_{po}(T)$ and imaginary $C''_{po}(T)$ components of $C_{po}^*(T)$ obtained on maltitol (a) and sorbitol (b), upon decreasing the temperature with the linear rate $q = -0.1$ K min⁻¹ and for periods of temperature modulation in the range of 20–100 s. The enthalpic relaxation times $\tau(T_\omega) = 1/\omega$ (where ω is the pulsation of the modulated temperature) are determined by TMDSC from the temperature T_ω of the peak maximum and are reported in the Arrhenius plots (open squares in Figure 4a,b). It allows us to extend the determination of the relaxation times close to T_g .

IV. Isothermal Measurements of the Sub- T_g Processes in Maltitol

To characterize in detail the R_1 and R_2 processes and their possible link to molecular complexity, we have performed

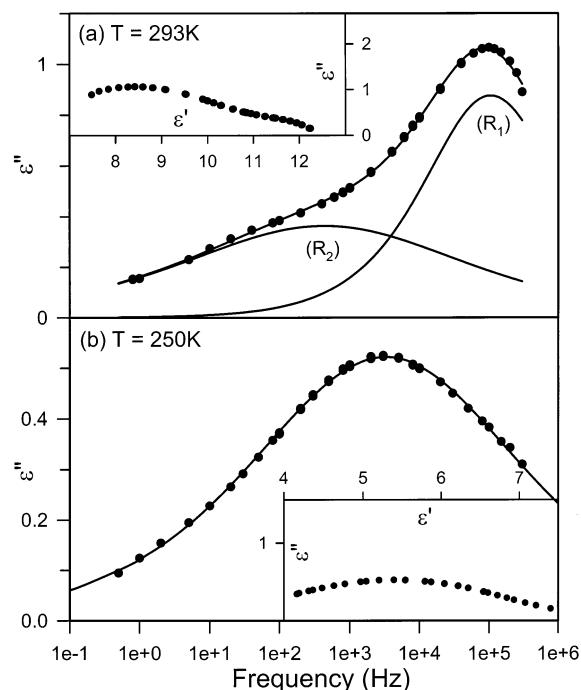


Figure 3. Imaginary part of the dielectric susceptibility of (a) maltitol and (b) sorbitol vs frequency at $T_g - 20$ K. The data for maltitol are fitted with two Cole–Cole relaxation functions, and the solid line is the sum of the two fitted Cole–Cole functions. Inserts: normalized Cole–Cole diagrams.

parallel isothermal investigations of the secondary processes of maltitol and sorbitol. The complex dielectric response $\epsilon^*(\omega)$ has been recorded over an effective frequency range of six decades (1 Hz; 300 kHz) at various temperatures below their respective glass transition temperature.²³ Contrary to the α process, the sub- T_g relaxation processes can be investigated isothermally. The dielectric loss $\epsilon''(\omega)$ of maltitol at room temperature ($T_g - 20$ K) is displayed in Figure 3a. The complexity of the relaxation processes occurring below T_g is revealed by a noticeable shoulder on the low-frequency side of the relaxation peak. The two contributions are also seen on the Cole–Cole diagram (Figure 3a inset), which can only be understood as a result of the combination of two arcs. The real and imaginary parts of the dielectric response are well-described by the superposition of two Cole–Cole relaxation functions:

$$\epsilon^*(\omega) = \sum_{i=1,2} \epsilon_{i\infty} + \frac{\Delta\epsilon_i}{1 + (i\omega\tau_i)^{(1-\alpha_i)}} \quad (1)$$

where α_i is a parameter connected to the broadening of each component in the spectrum ($\alpha_i = 0$ corresponds to the case of a Debye process exhibiting the characteristic full width at half-maximum of 1.14 decades). τ_1 and τ_2 are the relaxation times associated, respectively, with the R_1 and R_2 processes, and the value of the α_i parameter is found about twice for the broadest R_2 contribution than for the R_1 (at 293 K, $\alpha_1 = 0.4$ and $\alpha_2 = 0.7$). The temperature evolution of the relaxation times resulting from the refinement is displayed in the Arrhenius plot (Figure 4a).

V. Relaxation in Sorbitol

Isothermal measurements of sorbitol have been performed on a large range of temperatures, from 313 K down to 200 K ($T_g \approx 270$ K). Noticeable changes in comparison with maltitol

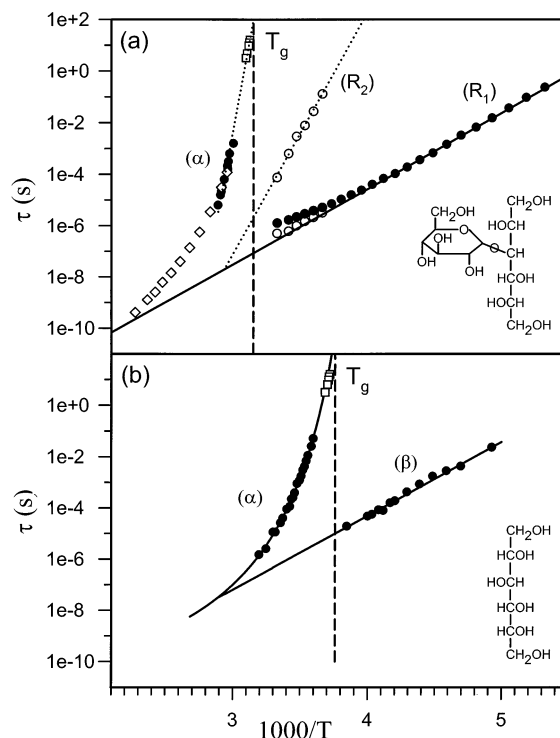


Figure 4. Arrhenius plot of the relaxation times of (a) maltitol. Full circles describing the α process are determined from the maximum loss peak during isochronal measurements. R_1 and R_2 processes are characterized by isothermal measurements: the full circles correspond to the frequency of the maximum loss peak, and open circles refer to the relaxation time determined with the fit on two Cole–Cole functions. Viscosity (open diamond) and modulated DSC data (open squares) from ref 28 are also reported. (b) Sorbitol. The solid lines represent the fitting Arrhenius and VFT equations.

are observed on their respective sub- T_g spectra. The imaginary part of the dielectric response obtained for a temperature located 20 K below T_g is displayed in Figure 3b. Opposite to maltitol, sorbitol exhibits a unique broad relaxation process below its calorimetric glass transition. At $T = 250$ K, the Cole–Cole representation gives a single symmetrical and flat arc of a circle (Figure 3b inset). This also allows us to compare it with the spectrum of maltitol (Figure 3a) for the same temperature gap of 20 K with regard to their respective T_g values. Because T_g defines the same time scale for the main α relaxations in both glasses, the difference in peak frequency of secondary processes as shown in Figure 3a,b indicates that the merging of the main and secondary processes in the two compounds will certainly not occur on the same time scale. The sub- T_g spectrum of sorbitol appears as a very broad and symmetric spectrum whose width covers the corresponding frequency range of the whole of the R_1 and R_2 processes. The analysis of the dielectric response in terms of one Cole–Cole relaxation function (eq 1) gives a broadening parameter $\alpha = 0.69$. The temperature evolution of the fitted relaxation times of the secondary processes is reported on the Arrhenius plot of Figure 4b. We also report data obtained above T_g , which are related to the primary α relaxation.

VI. Discussion

Figure 4a gathers together the temperature evolutions of the relaxation times of the different processes observed in maltitol (α , R_1 , R_2) from both isothermal and isochronal measurements. Concerning the α process, there is a perfect continuity in the temperature evolutions of the dielectric and specific heat

spectroscopy data both obtained in an isochronal way. On the narrow accessible high-temperature range, the most probable relaxation time of the main α process follows the Arrhenius law, explicitly $\tau(T) = \tau_0 \exp(E_\alpha/T)$ with $E_\alpha = 52\,770$ K and $\tau_0 = 3.1 \times 10^{-72}$ s. Such values indicate that the overall evolution of the dynamics of the glass former must be certainly strongly nonArrhenius. An attempt to analyze the temperature evolution of this process using a Vogel–Fülcher–Tamman (VFT) equation is hampered by the impossibility to cover many decades of frequency on the high-temperature side of the plot. The extrapolated relaxation time of the α process is about 10^2 s at the calorimetric glass transition temperature. Specific heat and dielectric spectroscopies thus probe the same structural relaxation modes, which are arrested at T_g on the experimental time scale. Isothermal investigations of the sub- T_g relaxations yield a temperature change of the relaxation time measured at the peak, which is represented by full circles in Figure 4a. At the lowest temperatures, data exhibit an Arrhenius dependence of the relaxation times. However, an unphysical upward departure from the Arrhenius line is observed when approaching T_g . This is an artifact of determining only the most probable time τ (maximum of $\epsilon''(\omega)$). It can be resolved by analyzing the temperature dependence of the two processes R_1 and R_2 described above. The results of the fit of the loss peak with two processes (eq 1) are displayed by open circles. Both processes seems to show a thermally activated behavior. The energy barrier E and the preexponential factor τ_0 are determined as $E_2 = 21\,800$ K, $\tau_0(R_2) = 10^{-35}$ s for the R_2 process and $E_1 = 6800$ K, $\tau_0(R_1) = 10^{-16}$ s for the R_1 process. The lowest activated R_1 process is thus expected to have an Arrhenius behavior on a large temperature domain. It can be envisaged as being of the Johari–Goldstein type. The lower amplitude R_2 process is much more activated and could be expected to have a VFT behavior on a larger temperature range. This R_2 process thus appears to involve collective molecular relaxations as a main process usually does. From the condition $\tau_{R_2}(T_g) = 100$ s, one could even expect a second thermodynamic glass transition associated to the involved motions near 250 K. However, from the relative amplitude of the different processes, it clearly appears that the filiation between main and secondary processes concerns α and R_1 rather than R_2 and R_1 if one considers R_2 as a main process. Mechanical spectroscopic experiments performed in a higher time range¹⁷ ($\tau > 10^{-2}$ s) reveal main and secondary processes, which are an exact extrapolation of the dielectric data for α and R_1 , respectively. However, there is no signaled trace of a R_2 type process in the mechanical measurements. No process of R_2 type was detected either in previous dielectric measurements.¹⁴ The confrontation of the dynamical properties of maltitol and sorbitol reveals interesting features on the relaxation mechanisms of these two compounds. The α process of sorbitol shows a clear curvature in the Arrhenius plot (Figure 4b) and can be described by a VFT equation $\tau(T) = \tau_0 \exp[A/(T - T_0)]$. The resulting parameters are $\tau_0 = 4 \times 10^{-12}$ s, $A = 961$ K, and $T_0 = 236.5$ K. The Arrhenius parameters describing the β relaxation are $E = 6640$ K and $\tau_0 = 10^{-16}$ s in agreement with the analysis of previously published dielectric^{14,18,19} and mechanical¹⁷ data. The most striking feature revealed by Figure 4 is that the relaxation times of the secondary processes of maltitol (R_1) and sorbitol (β) have exactly similar values at all investigated temperatures and are thus characterized by the same activation energy. This indicates that the secondary process of maltitol cannot be attributed to local motions of the side cycle. The superposition of the Arrhenius laws of the secondary processes in the two

systems also strongly suggests that the same microscopic process or the same species contribute to the Johari–Goldstein type relaxation mechanism. The lowest activated relaxation processes are thus independent of the respective molecular complexity of both compounds whereas the primary relaxation process and the glass transition temperature are dependent on the molecular weight. As a consequence, primary and secondary relaxation processes bifurcate on different time scales (t_b (sorbitol) = 10^{-8} s; t_b (maltitol) = 10^{-10} s). This difference is also observed on their respective relaxation time at T_g (τ_{β,T_g} (sorbitol) = 10^{-5} s; τ_{β,T_g} (maltitol) = 10^{-7} s). The existence of a correlation between the value τ_{β,T_g} and the KWW exponent β_{KWW} of the α relaxation has been pointed out by Ngai.³² The possibility to determine β_{KWW} from TMDSC measurements has been shown in ref 22. This is especially useful in the case of maltitol for which no low-frequency dielectric data are available. We have obtained β_{KWW} (sorbitol) = 0.55 and β_{KWW} (maltitol) = 0.48. This conforms to the trend expected from the coupling model that the smaller Kohlraush exponent of the α relaxation tends to have shorter β relaxation time $\tau_\beta(T_g)$. Mechanisms involving OH bonds breaking are primarily suspected for being implied in the β relaxation of both compounds, and the high dielectric strength is certainly related to the large number of implied units. However, as it was recognized previously for sorbitol,¹⁸ the abnormally high activation energy cannot be connected to motions of individual hydroxyl (OH) or methylol (CH₂OH) groups. The presence of the side ring is suspected to be at the origin of the additional R_2 process in maltitol. The existence of several sub- T_g relaxation processes has been signaled in disaccharides cellobiose and gentiobiose³³ having the same glucopyranose ring as maltitol. In these cases, a quasi-Debye process, called “ γ ”, has been observed in addition to a strongly distributed β relaxation process. However, this γ process is found at higher frequency than β and is characterized by a low activation energy ($E_\gamma = 2300$ K). It has been assigned to the fast rotation mobility of the different methylol and hydroxyl side groups. Such a process should be observed in maltitol but at high frequency/low temperature (not accessible with our equipment). Because the R_2 process is highly activated, it must be ascribed to a high degree of cooperativity, which continues to develop below T_g . The origin of the R_2 process would thus involve mainly intermolecular bonds and result from coupled rotation of the rings. A relevant example is the cooperative dynamics of the β process of the mesogenic groups (two phenyl rings) in a side chain liquid crystalline polymer.³⁴ However, the mechanism by which a cooperativity involving preferentially the side ring motions could continue to proceed while the main process is frozen in, is unclear in maltitol, all the more that there is no equivalence of the R_2 process in the two mentioned disaccharides. Emergence of plural α processes has yet been detected in molecular liquids^{4,5,18} and glassy crystal cyclohexanol.¹¹ However, in that case, similar decoupling was also observed at the level of the β processes. This is not the case in maltitol, where only one secondary β process exists.

Figure 3a,b reveals noticeable relationships between the secondary processes in both polyols. Whereas sorbitol gives rise to a very broad single peak of β relaxation, maltitol exhibits a bimodal (R_1 , R_2) distribution. At the same temperature, the maximum of R_1 exactly corresponds to the maximum of β in sorbitol (Figure 4). They may thus be attributed fundamentally to the same relaxation process with identity of their most probable relaxation time. A salient feature is that R_1 is much sharper than β . It looks as if some contributions to the β relaxation in sorbitol were suppressed by the mechanism giving

rise to R_2 . Because of its higher molecular complexity, maltitol favors the possibility of formation of intramolecular bonds. If the origin of the β relaxation was intramolecular in nature, one would expect a sharper peak in sorbitol, which is not the case. This suggests that the contribution to the (β , R_1) relaxations mainly involves intermolecular bonds through methylol and hydroxyl groups, some of these interactions being suppressed in maltitol to the benefit of highly cooperative interring processes. At this level, it is interesting to compare these results with the results of a recent investigation of the two polyols by thermally stimulated depolarization current (TSDC) technique.³⁵ The components of the different relaxations can be observed when they enter in the time window of this selective technique. The β – α branching of sorbitol could thus be observed at the level of the wings of their distributions. It was shown that the relaxation times of the two processes are close enough for the higher temperature components of the β relaxation and the lower temperature components of the α relaxation to appear in the same temperature range (≈ 240 K). Such an overlap is not observed in maltitol as a consequence of the α and β processes being more apart. The analysis of the processes in terms of activation enthalpy and entropy definitely demonstrates that the relaxation processes detectable at the lower temperature in both compounds show a zero entropy behavior. Otherwise stated, the corresponding behaviors are noncooperative. In maltitol, the TSDC technique reveals a temperature gap (≈ 250 – 280 K) between the β (or equivalently named R_1) process and the highly activated α process. Most of this gap arises from the fact that any appreciable polarization cannot be created. However, some trend to develop an intermediate thermally stimulated component with a nonzero entropy contribution is revealed. It could coincide with the presence of the intermediate R_2 process presently observed.

Acknowledgment. This work has benefited from the help of the Nord-Pas de Calais region in the frame of the genopole program.

References and Notes

- (1) Johari, G. P. *Ann. N. Y. Acad. Sci.* **1976**, 279, 117.
- (2) Ngai, K. L. *Phys. Rev. E* **1998**, 57, 7346.

- (3) Hansen, C.; Stickel, F.; Berger, T.; Richert, R.; Fischer, E. W. *J. Chem. Phys.* **1997**, 107, 1086.
- (4) Murthy, S. S. N.; Sobhanadri, J.; Gangasharan. *J. Chem. Phys.* **1993**, 100, 4601.
- (5) Gangasharan; Murthy, S. S. N. *J. Chem. Phys.* **1993**, 99, 9865.
- (6) Casalini, R.; Fioretto, D.; Livi, A.; Lucchesi, M.; Rolla, P. A. *Phys. Rev. B* **1997**, 56, 3016.
- (7) Deegan, R. D.; Nagel, S. R. *Phys. Rev. B* **1995**, 52, 5653.
- (8) Johari, G. P.; Goodby, J. W. *J. Chem. Phys.* **1982**, 77, 5165.
- (9) Adachi, K.; Suga, H.; Seki, S.; Kubota, S.; Yamaguchi, S.; Yano, O.; Wada, Y. *Mol. Cryst. Liq. Cryst.* **1972**, 18, 345.
- (10) Böhmer, R.; Angell, C. A. In *Disorder Effects on Relaxational Processes*; Richert, R., Blumen, A., Eds.; Springer-Verlag: New York, 1994.
- (11) Mizukami, M.; Fujimori, H.; Oguni, M. *Solid State Commun.* **1996**, 100, 83.
- (12) Margulies, M. M.; Sixou, B.; David, L.; Vigier, G.; Dolmazon, R.; Albrand, M. *Eur. Phys. J. E* **2000**, 3, 55.
- (13) Fujima, T.; Frusawa, H.; Ito, K.; Hayakawa, R. *Jpn. J. Appl. Phys.* **2000**, 39, L744.
- (14) Faivre, A.; Niquet, G.; Maglione, M.; Fornazero, J.; Jal, J. F.; David, L. *Eur. Phys. J. B* **1999**, 10, 277.
- (15) Nakheli, A.; Eljazouli, A.; Elmorabit, M.; Ballouki, E.; Fornazero, J.; Huck, J. *J. Phys. C* **1999**, 11, 7977.
- (16) Nozaki, R.; Suzuki, D.; Osawa, S.; Shiozaki, Y. *J. Non-Cryst. Solids* **1998**, 235–237, 393.
- (17) Faivre, A.; David, L.; Perez, J. *J. Phys. II* **1997**, 7, 1635.
- (18) Murthy, S. S. N. *Mol. Phys.* **1996**, 87, 691.
- (19) Angell, C. A.; Smith, D. L. *J. Phys. Chem.* **1982**, 86, 3845.
- (20) Olsen, N. B. *J. Non-Cryst. Solids* **1998**, 235–237, 399.
- (21) Wagner, H.; Richert, R. *J. Phys. Chem. B* **1999**, 103, 4071.
- (22) Carpentier, L.; Bustin, O.; Descamps, M. *J. Phys. D* **2002**, 35, 402.
- (23) Sinito, M. Thésis, Lyon, France, 1995.
- (24) McCrum, N. G.; Read, R. E.; Williams, G. *Anelastic and Dielectric Effects in Polymeric Solids*; Wiley: London, 1967.
- (25) Johari, G. P.; Goldstein, M. *J. Chem. Phys.* **1970**, 53, 2372.
- (26) Wu, L.; *Phys. Rev. B* **1991**, 43, 9906.
- (27) Böhmer, R.; Ngai, K. L.; Angell, C. A.; Plazcek, D. J. *J. Chem. Phys.* **1993**, 99, 4201.
- (28) Bustin, O.; Descamps, M. *J. Chem. Phys.* **1999**, 111, 10982.
- (29) Schawe, J. E. K. *Thermochim. Acta* **1995**, 260, 1.
- (30) Hutchinson, J. M. *Thermochim. Acta* **1998**, 324, 165.
- (31) Carpentier, L.; Bourgeois, L.; Descamps, M. *J. Therm. Anal.* **2002**, 68, 727.
- (32) Ngai, K. L. *J. Chem. Phys.* **1998**, 109, 6982.
- (33) Einfeldt, J.; Meisner, D.; Kwasniewski, A. *Prog. Polym. Sci.* **2001**, 26, 1419.
- (34) Ngai, K. L.; Schönhals, A. *J. Polym. Sci. Polym. Phys.* **1998**, 36, 1927.
- (35) Correia, N. T.; Alvarez, C.; Ramos, J. M.; Descamps, M. *J. Phys. Chem. B* **2001**, 105, 5663.